A Cortical Extracellular Simulation Model to Create Synthetic Neural Recordings

Kyle Gherardi and Hakan Töreyin

Abstract— **Synthetic extracellular neural recordings allow precise knowledge of when and which neuron spikes in a recording, and therefore are important to assess and refine spike detection and sorting algorithms. Such algorithms are strongly dependent on the spike waveform shapes. Therefore, it is critical for a model that generates synthetic recordings to incorporate the factors changing the waveform shape in the neural environment. In this paper, we present a simulation tool that models frequency-filtering and layer-inhomogeneity of cortical layers, where most actual extracellular recordings are performed. The tool uses simulated transmembrane currents of neurons from NEURON, and implements line-source-approximation, method-of-images, and low-pass filtering to calculate the potentials on MATLAB.**

I. Introduction

Information is represented by means of neural spikes in the brain. Therefore, by monitoring the spiking activity in the brain, connectivity of the brain and computations performed can be explored. The most direct way of neural activity monitoring involves analyzing the neural spikes captured as electrical potentials by electrodes placed in extracellular neural tissue. A striking application of neural signal analysis is brain-computer interfaces (BCI), where the spikes of pyramidal neurons in the brain cortex are decoded into high-level information such as movement inference. Neural spike analysis aims extracting the activities of different neurons nearby a recording electrode and typically involves spike detection and sorting steps. In the literature, various algorithms have been proposed towards improving the accuracy of spike detection and sorting [1,2,3].

To properly assess the performance of an algorithm, biological extracellular recordings are widely used [5]. In these datasets, precise knowledge of neuron firing information, which is critical to assess spike sorting performance, is obtained via simultaneous intracellular recordings. The challenges in performing intracellular recordings impose a limit on maximum the number of neurons whose activities could be precisely known. To overcome the challenge in biological recordings, different research groups have proposed models for generating synthetic datasets [1,2,3]. Synthetic datasets offer the advantage of precise firing information knowledge for large numbers of neurons. Clearly, a synthetic dataset needs to faithfully emulate a biological recording. Specifically, in the context of spike detection and sorting; accurate modeling of spike waveform shapes, activity levels of neurons, and background noise are critical.

The latter two, activity levels and background noise, are well-characterized and therefore realistically simulated in existing models in the literature. On the other hand, the extracellular spike waveform shape of a firing neuron is impacted by several factors such as the transmembrane current profiles of the neuron, the geometrical properties such as distance and orientation of the neuron with respect to the electrode, the electrode dimensions and electrical model, and the impedance profile of the neural tissue. Previous models have reflected the impacts of biophysical and geometrical properties of neurons as well as the electrode properties on spike waveforms [1,2,3].

On the other hand, these models do not offer a comprehensive impedance modelling of the brain cortex. First, in some of these models, brain cortex is represented as a single homogeneous medium [1,2,3], which does not accurately reflect the multi-layered structure of the cortex. Notably, due to the nonlinearities introduced on current paths by boundaries between different layers, the relationship between the transmembrane currents and the resultant extracellular potential does not solely depend on the distance [4]. Second, in some [2,3], the tissue is modeled using a constant conductivity, thereby neglecting the low-pass-filtering effect of the tissue.

To accurately incorporate the effects of brain cortex impedance properties on the extracellular waveform shapes, and therefore obtain more realistic synthetic datasets, in this study we present a new extracellular medium simulation tool.

II. Methods

An overview of our simulation approach is presented in Fig. 1. First, we use the NEURON software [5] to simulate the transmembrane currents for each compartment of a neuron. Our NEURON model generates the transmembrane currents based on the defined biophysics and geometrical information provided for the different sections of a neuron; namely dendrite, soma, and axon; and the excitation method of the neuron. To simulate the response to a natural excitation of neurons (i.e., conductance-change in a postsynaptic neuron), we used NEURON's Alpha Synapse. The transmembrane current simulations of neurons with different biophysical, geometrical, and/or connectivity-related properties are performed by changing those properties on a single .hoc file run on NEURON. Lastly, we parse the NEURON data to

*This material is based upon work supported by the National Science Foundation under Grant Number 1916160.

K. Gherardi is with San Diego State University, San Diego, CA 92182 USA (e-mail: kgherardi@sdsu.edu).

H. Töreyin is with San Diego State University, San Diego, CA 92182 USA. (phone: 619-594-0795; e-mail: htoreyin@sdsu.edu).

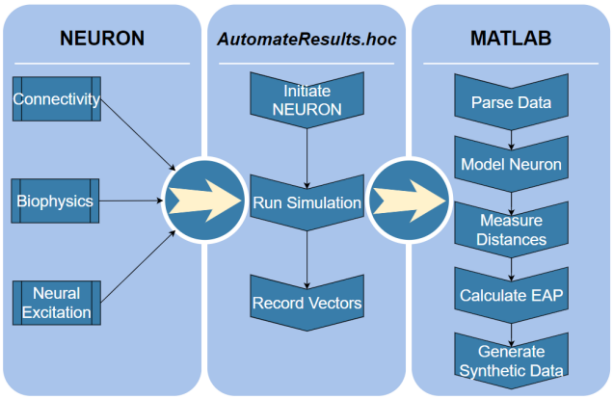

Figure 1. Flowchart of the computer model.

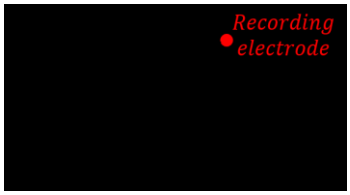

Figure 2. A line current source and the distances to a recording electrode.

MATLAB, where we generate the synthetic data based on a hypothetical neuron distribution around a recording electrode in a double layer cortex tissue.

The principles of simulating extracellular potentials are as follows. When a neuron membrane potential exceeds the threshold and fires a spike, the channels of the membrane that are in a small proximity will let Na^{+1} and K^{+1} ions to move across the membrane, and thus resulting in ionic currents. Volume conduction of the ionic transmembrane currents results in an electrical potential on an electrode placed at an extracellular location. An extracellular medium having multiple current sources, each belonging to a different segment of a different neuron, can be considered as a linear time invariant system (LTI). An LTI system allows the use of superposition principle to calculate the contribution of each current source on an extracellular potential recorded by an electrode.

In an extracellular space, a point current source, $+I$, will spread radially from the source. Based on the conservation of charge and the Ohm's law, in a homogeneous medium having a constant conductivity, σ, it can be shown that the electric field, E, and the resultant extracellular potential, V_{ps}, due to volume conduction are respectively:

$$E(R) = \frac{I}{4\pi\sigma R^2}, \tag{1}$$

$$V_{ps} = -\int_{R}^{\infty} E(R')\,dR' = \frac{I}{4\pi\sigma R}\ , \tag{2}$$

where R is the distance from the point source. Our model assumes the soma as a point source. For neurites (i.e., dendrite and axon), the result in equation (*2*) can be expanded to a 2D neuron through line-source approximation (LSA) by leveraging the cylindrical coordinate system [6]. In LSA, neurites are divided into smaller segments used as independent line current sources. On each segment, a uniform

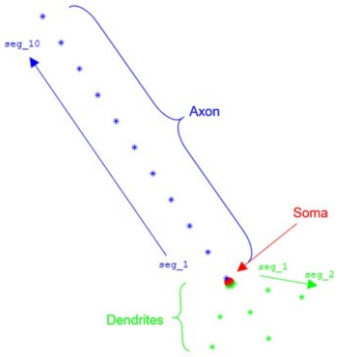

Figure 3. The neuron connectivity used in this study. The axon and each dendrite branch are divided into ten and two segments, respectively.

line current distribution is assumed, where the current is the sum of transmembrane currents corresponding to different ions In this analysis, for a line current source with a length of Δs (Fig. 2), corresponding extracellular potential, V_{ls}, is calculated as [6]:

$$V_{ls} = \frac{V_{ps}}{\Delta s}\begin{cases} \log\dfrac{\sqrt{h^2+r^2}-h}{\sqrt{l^2+r^2}-l} & Case1 \\ \log\dfrac{\left(\sqrt{h^2+r^2}-h\right)\left(\sqrt{l^2+r^2}+l\right)}{r^2} & Case2 \\ \log\dfrac{\sqrt{l^2+r^2}+l}{\sqrt{h^2+r^2}+h} & Case3 \end{cases} \tag{3}$$

The distances, *h,r,* and *l* are shown in Fig. 2. In equation (3); Case1 is $h,l < 0$; Case2 is $h<0$, $l>0$; and Case3 is $h,l>0$. The neuron connectivity used in this study is presented in Fig. 3.

A. Low-Level Simulations on NEURON

We use the NEURON software to simulate the transmembrane currents for soma and neurites. We use passive membrane modeling for the dendrite and active Hodgkin-Huxley modeling for the soma and the axon. For a dendrite and axon segment, simulated current waveforms corresponding to two different channel conductance values and capacitive nature of the neural membrane are presented in Fig. 4. The waveforms demonstrated how the current amplitude varies with the channel conductance of the corresponding ion. We used conductance values that lie within the biological ranges for pyramidal cells [5].

B. High-Level Simulations on MATLAB

The neuron-level simulation data from NEURON are used to calculate an extracellular potential recording for a hypothetical extracellular recording medium. To define a hypothetical medium; we identify neuron-related properties such as the number of neurons, distance and orientation of neurons with respect to the electrode; and the position of the boundary between different cortical layers.

Modeling frequency-dependent volume conduction: Equations (2) and (3) reflect the distance dependence of the extracellular potential. However, the approximation of constant conductivity neglects the frequency dependence of the medium originated from the spatial inhomogeneities in conductivity and permittivity. In reality, the extracellular medium introduces low-pass filtering effect due to the spatial

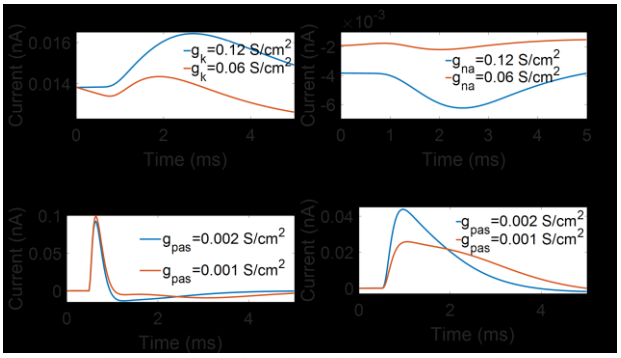

Figure 4. Effects of channel conductivities on transmembrane currents for an actively (axon) and passively (dendrite) simulated neurite segment.

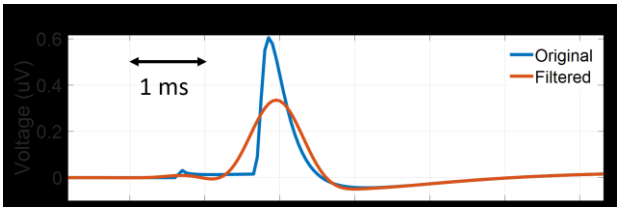

Figure 5. The frequency-dependence of the medium is reflected into the model as a 1st order low-pass filter.

inhomogeneities in conductivity and permittivity, which can be modeled as a 1st order low-pass filter [7]. For biologically realistic values, the low-pass filter has a cut-off frequency of ~100 Hz [8]. Beginning with equations (2) and (3) the extracellular potential, V_{ext}, is calculated and then applied to the low-pass filter. The smoothing effect of the filter is shown in Fig. 5.

Modeling layer inhomogeneity: The cerebral cortex consists of six layers (L1-through-L6) that differ in terms of neuron distribution and connectivity. Accordingly, the impedance characteristics of the extracellular medium varies from layer to layer, thereby creating discontinuity in conductivities at the layer boundaries [9]. In such an inhomogeneous medium, layer boundaries will cause nonlinearities in the spread of the current, and therefore distort the resultant V_{ext}. A precise modeling of the current spread can be performed by solving the Poisson's equation via finite-element-analysis (FEA) tools. On the other hand, two properties of the inhomogeneity allow us to leverage a computationally efficient analytical solution, alternative to FEA, namely method-of-images (MoI). The first property is that the cortical layers extend almost parallel to each other and therefore the conductivity inhomogeneity is in the z-direction. Second, the neuron-electrode distance where a neural spike becomes equal to the noise floor and thus can barely be detected is ~140 µm [10]. Considering the layer thickness ranges of ~200 µm (L2) to ~700 µm (L3) [11], the inhomogeneity in a practical extracellular recording would be created by two layers only. An illustration of an electrode, the circular region in which neural activities can be collected from, and different cortical layers are shown in Fig. 6. The MoI is applied by assuming an image of the source in the other layer such that the continuity of the tangential and perpendicular components of the E field are satisfied at the boundary [12]. The source and image neuron-electrode

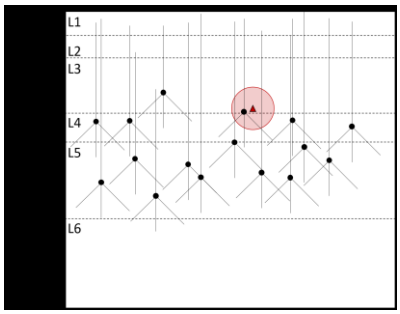

Figure 6. The region within which neural spikes can be detected (red circular region) is illustrated for an electrode (red triangle) placed in L3 of the cortical tissue.

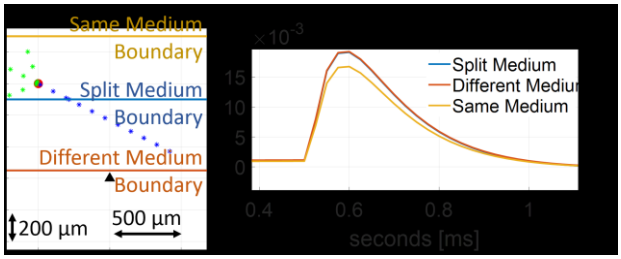

Figure 7. Depending on where the layer boundary is, the spike of a neuron would result in a different spike waveform at the electrode. For three boundary locations on the left, the waveforms are shown on the right.

distances are modeled by the coordinate pair *(x,y)* and *(x',y')* respectively, as in equations (4) and (5). For the case when the electrode and the current source are in the same cortical layer, the extracellular potential, V_{ext}, is:

$$V_{ext} = V_{source}(x,y) + r_2 V_{image}(x',y'), \quad (4)$$

where the reflection coefficient due to the second layer $r_2 = \frac{\sigma_1-\sigma_2}{\sigma_1+\sigma_2}$, and σ_1 and σ_2 are the conductivities of the first and second medium respectively. When the electrode and the current source are in different layers:

$$V_{ext} = t_2 V_{source}(x,y), \quad (5)$$

where the transmission coefficient due to the second layer $t_2 = \frac{2\sigma_1}{\sigma_1+\sigma_2}$. The location of where the layer boundary is, changes V_{ext} for a given electrode-neuron placement, as illustrated in Fig. 7.

Extracellular medium generation and integrating the contributions from the line segments: Our model arbitrarily places neurons and the boundary layer around an electrode positioned at the coordinates (0,0). The model mimics the vertical alignment of the pyramidal cells along the cortex. An example placement is shown in Fig. 8. Note that in Fig. 8, the same color code in Fig. 3 is used to denote the neurites.

Next, the model calculates the distances (i.e., h, r, and l) for each compartment with respect to the recording electrode and determines if the segment is in the same or opposite layer with respect to the layer that the electrode is in. The transmembrane current, extracellular conductivity, and the calculated distances are used in equations (2-3) to equate the electric potential contribution for each compartment, which when compiled develops the electric potential for each neuron.

The electric potential calculation is repeated for all neurons within the virtual environment. Firing rates are arbitrarily

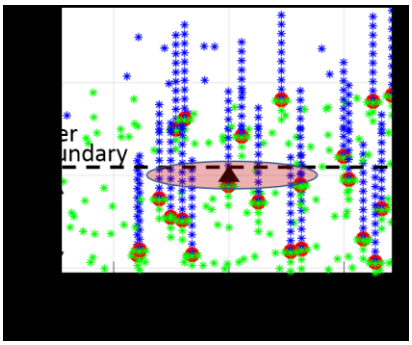

Figure 8. An example neuron distribution around an electrode (black triangle). Note the different scales in the x (200 µm/square) and y (1000 µm/square) axes. The region within which spike activity can be detected is shown as the red elliptical region. A layer boundary crosses the region.

assigned to each neuron, which are then sequenced pseudo-randomly and triggered to fire throughout the specified duration, thus creating a compiled synthetic data sequence. The background noise is simulated as a combination of white and flicker noise based on [13].

III. Example Synthetic Data

We created a 60 s synthetic extracellular recording using the proposed model with ten randomly selected neurons. The dataset is presented in Fig. 9. Simulations were performed on a 64-bit Windows PC with Intel 8th Generation processor and 12 GB of RAM. The simulations took 4.85 s.

IV. Discussion

A summary of the proposed simulation tool and comparison with recent alternative tools are provided in Table I. The table is prepared with the consideration of metrics that impact the spike waveform shapes and thus are important for spike detection and sorting applications. All tools in the table use NEURON to simulate the transmembrane currents. What differentiates the proposed simulator from the others is the ability to model both frequency-dependence and inhomogeneity of the cortical layers. The synthetic data presented in Fig. 9 is created using a simple neuron connectivity shown in Fig. 3. However, the tool allows use of neurons with more complicated connectivity such as in [14]. To more accurately model an actual extracellular recording, future improvements will include incorporating the effects of electrode properties and medium anisotropies.

V. Conclusion

We presented a simulation tool to create synthetic extracellular neural recordings. Its ability to model the conductivity inhomogeneities and frequency-dependences in the simulated environment distinguishes it from the alternatives and makes it convenient for investigating new spike detection and sorting algorithms such as [15-16].

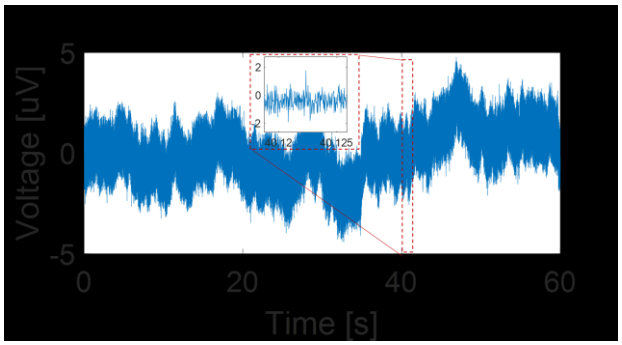

Figure 9. An example 60 s synthetic dataset. A spike is highlighted.

TABLE I. Comparison With Other Tools

	This Work	LFPsim (2016) **[1]**	Bionet (2018) **[2]**	LFPY2 (2018) **[3]**
Model Environment	MATLAB	NEURON	Python	Python
Frequency Dependence	Yes	Yes	No	No
Cortical Layer Inhomogeneity	Yes	No	No	No*
Anisotropy	No	No	No	Yes**
Electrode Model	No	No	No	Yes

*Models inhomogeneity for different head layers (e.g., skull, scalp).
**Models anisotropy for a homogeneous medium.

References

[1] Parasuram, Harilal, et al. "Computational modeling of single neuron extracellular electric potentials and network local field potentials using LFPsim." Frontiers in Computational Neuroscience 10 (2016): 65.

[2] Gratiy, Sergey L., et al. "BioNet: A Python interface to NEURON for modeling large-scale networks." PLoS One 13.8 (2018): e0201630.

[3] Hagen, Espen, et al. "Multimodal modeling of neural network activity: computing LFP, ECoG, EEG, and MEG signals with LFPy 2.0." Frontiers in neuroinformatics 12 (2018): 92.

[4] Nunez, Paul L., and Ramesh Srinivasan. Electric fields of the brain: the neurophysics of EEG. Oxford University Press, USA, 2006.

[5] Carnevale, N.T. and Hines, M.L. The NEURON Book. Cambridge, UK: Cambridge University Press, 2006.

[6] Holt, Gary R., and Christof Koch. "Electrical interactions via the extracellular potential near cell bodies." Journal of computational neuroscience 6, no. 2 (1999): 169-184.

[7] Bédard, Claude, Helmut Kröger, and Alain Destexhe. "Modeling extracellular field potentials and the frequency-filtering properties of extracellular space." Biophysical journal 86, no. 3 (2004): 1829-1842.

[8] Bédard, Claude, Helmut Kröger, and Alain Destexhe. "Model of low-pass filtering of local field potentials in brain tissue." Physical Review E 73, no. 5 (2006): 051911.

[9] Goto, Takakuni, et al. "An evaluation of the conductivity profile in the somatosensory barrel cortex of Wistar rats." Journal of neurophysiology 104.6 (2010): 3388-3412.

[10] Maguire, Yael G., et al. "Physical principles for scalable neural recording." Frontiers in computational neuroscience 7 (2013): 137.

[11] DeFelipe, Javier, Lidia Alonso-Nanclares, and Jon I. Arellano. "Microstructure of the neocortex: comparative aspects." Journal of neurocytology 31.3-5 (2002): 299-316.

[12] Dias, C. J., and R. Igreja. "A method of recursive images to obtain the potential, the electric field and capacitance in multi-layer interdigitated electrode (IDE) sensors." Sensors and Actuators A: Physical 256 (2017): 95-106.

[13] Musial, P. G., et al. "Signal-to-noise ratio improvement in multiple electrode recording." Journal of neuroscience methods 115, no. 1 (2002): 29-43.

[14] Mainen, Zachary F., and Terrence J. Sejnowski. "Influence of dendritic structure on firing pattern in model neocortical neurons." Nature 382.6589 (1996): 363-366.

[15] Franke, Felix, et al. "Bayes optimal template matching for spike sorting–combining fisher discriminant analysis with optimal filtering." Journal of computational neuroscience 38, no. 3 (2015): 439-459.

[16] Güngör, Cihan Berk, and Hakan Töreyin. "Facilitating stochastic resonance as a pre-emphasis method for neural spike detection." Journal of Neural Engineering 17, no. 4 (2020): 046047.